Published in final edited form as:

Sci Transl Med. 2018 November 21; 10(468): . doi:10.1126/scitranslmed.aau0670.

Long term mechanical function and integration of an implanted tissue engineered intervertebral disc

Sarah E. Gullbrand[1,2], **Beth G. Ashinsky**[1,2,3,†], **Edward D. Bonnevie**[1,2,†], **Dong Hwa Kim**[1,2,†], **Julie B. Engiles**[6], **Lachlan J. Smith**[1,2,4], **Dawn M. Elliott**[5], **Thomas P. Schaer**[6], **Harvey E. Smith**[1,2,4,*], **Robert L. Mauck**[1,2,7,*]

[1]Translational Musculoskeletal Research Center, Corporal Michael J. Crescenz VA Medical Center, Philadelphia, PA, 19104, USA

[2]McKay Orthopaedic Research Laboratory, Department of Orthopaedic Surgery, Perelman School of Medicine, University of Pennsylvania, Philadelphia, PA, 19104, USA

[3]School of Biomedical Sciences, Drexel University, Philadelphia, PA, 19104, USA.

[4]Department of Neurosurgery, University of Pennsylvania, Philadelphia, PA, 19104, USA

[5]Department of Biomedical Engineering, University of Delaware, Newark, DE, 19716, USA

[6]Department of Clinical Studies, New Bolton Center, School of Veterinary Medicine, University of Pennsylvania, Philadelphia, PA, 19348, USA

[7]Department of Bioengineering, University of Pennsylvania, Philadelphia, PA, 19104, USA

Abstract

Tissue engineering holds great promise for the treatment of advanced intervertebral disc degeneration. However, assessment of in vivo integration and mechanical function of tissue engineered disc replacements over the long term, in large animal models, will be necessary to advance clinical translation. To that end, we developed tissue engineered, endplate-modified, disc-like angle ply structures (eDAPS) sized for the rat caudal and goat cervical spines that recapitulate the hierarchical structure of the native disc. Here, we demonstrate functional maturation and integration of these eDAPS in a rat caudal disc replacement model, with compressive mechanical properties reaching native values after 20 weeks in vivo and evidence of functional integration under physiologic loads. To further this therapy towards clinical translation, we implanted eDAPS sized for the human cervical disc space in a goat cervical disc replacement model. Our results demonstrate maintenance of eDAPS composition and structure up to 8 weeks in vivo in the goat cervical disc space, and maturation of compressive mechanical properties to match native levels.

*Corresponding Authors: lemauck@pennmedicine.upenn.edu, Harvey.Smith@uphs.upenn.edu.
†These authors contributed equally to this study and are listed alphabetically.

Author contributions: SEG: study design, *in vitro* assays, *in vivo* assays, data analysis, interpretation of results, manuscript preparation; BGA: *in vitro* assays, *in vivo* assays, data analysis; EB: *in vitro* assays, data analysis; DHK: *in vitro* assays; JBE: histo-pathological analysis, interpretation of results; LJS: study design, interpretation of results; TPS: *in vivo* assays; DME: study design, interpretation of results; HES: study design, *in vivo* assays, interpretation of results, manuscript preparation; RLM: study design, interpretation of results, manuscript preparation.

Competing interests: The authors declare no potential conflicts of interest with respect to the research, authorship and/or publication of this manuscript.

Data and materials availability. All data associated with this study are present in the paper or supplementary materials

These results demonstrate the translational feasibility of disc replacement with a tissue engineered construct for the treatment of advanced disc degeneration.

One Sentence Summary:

Tissue engineered intervertebral discs demonstrate long term functional integration in rat and goat disc replacement models.

Introduction

Back and neck pain are ubiquitous in modern society, affecting about one half of adults each year, and about two thirds of adults at some point in their lives.(1) Globally, back and neck pain are two of the top four contributors of years lived with disability, and treatment of these conditions has increased healthcare expenditures without evidence of improvement in patient health status.(2, 3) Although the causes of back pain are multifactorial and still not fully understood, degeneration of the intervertebral disc is frequently associated with axial spine pain and neurogenic extremity pain.(4) Intervertebral disc degeneration is characterized by a series of cellular, compositional, and structural changes, including loss of proteoglycan content in the nucleus pulposus (NP), cell death, disorganization of the annulus fibrosus (AF) and a collapse in disc height; together these changes ultimately compromise the mechanical function of the disc.(5, 6) Spinal fusion may be performed in patients with debilitating axial neck or back pain and a severely degenerated intervertebral disc; fusions are also commonly performed when it is necessary to remove the intervertebral disc to restore disc space height (indirectly decompressing the neural foramen) or to gain access to disc-osteophyte complexes that are narrowing the spinal canal. Spinal fusion does not restore native disc structure or mechanical function as it immobilizes the degenerative motion segment; this may contribute to the degeneration of adjacent motion segments due to alterations in whole spine kinematics.(7) Due in large part to the well-recognized clinical problem of adjacent segment degeneration, maintenance of intervertebral disc kinematics after discectomy or decompression of the disc with a mechanical arthroplasty device has emerged as an alternative to fusion procedures, with the goal of restoring disc height while preserving motion.(8) However, the widespread adoption of these devices has been slow, in part due to concerns over subsidence, wear particle generation, and the difficulty of revision surgery.(9–11)

Considering the social and economic burden of pain and disability associated with intervertebral disc degeneration, and the limitations of currently available surgical treatments, there is a substantial need for new therapies for advanced disc degeneration. Tissue engineering offers great promise – replacement of a degenerative disc with a tissue engineered composite disc has the potential to restore native disc structure, biology, and mechanical function. To date, a number of composite engineered intervertebral discs have been generated, generally involving the combination of a cell-seeded hydrogel (as an analog for the NP region) within a cell-seeded oriented or porous scaffold (as an analog for the AF region).(12–18) A variety of such composite discs have been characterized in vitro, though few studies have evaluated these constructs in vivo.(18–21) Understanding the long-term integration and mechanical function of engineered discs in vivo, especially in large animal

models at clinically relevant length scales, will be an essential pre-cursor for the translation of these engineered disc technologies into human clinical trials.

To address this, we developed endplate-modified disc-like angle ply structures (eDAPS) composed of three distinct components to mimic the hierarchical structure of the native spinal motion segment. The NP region is formed from a cell-seeded hyaluronic acid or agarose hydrogel, whereas the AF region is composed of cell-seeded, concentric layers of aligned, nanofibrous poly(ε-caprolactone) (PCL).(13, 22) Hydrogels were selected for the NP region to recapitulate the highly hydrated state of the native NP, whereas PCL was selected for the AF region due to its slow degradation rate, robust mechanical properties, and its ability to be fabricated via electrospinning into ordered structures that replicate the fiber architecture of the annulus fibrosus.(23–25) The AF and NP regions are combined with two acellular, porous PCL foams as endplate (EP) analogs to generate the eDAPS construct. We have previously evaluated these eDAPS in a rat caudal disc replacement model in short term studies, with endplate-modified constructs outperforming those without endplates.(21) Here, we demonstrate the long-term in vivo integration and mechanical function of eDAPS in the rat caudal spine. These engineered discs maintained composition and structure while functionally maturing in vivo, reaching near native tensile and compressive mechanical properties by 20 weeks. To further advance the clinical translation of tissue engineered disc replacements, we also successfully implanted human-sized eDAPS into the cervical spine of a large animal (caprine) model.

Results

eDAPS structure and composition are maintained in vivo.

To determine whether a tissue engineered disc can recapitulate the structure and function of the native disc with long-term implantation, eDAPS were implanted in vivo in a small animal disc replacement model for up to 20 weeks. eDAPS sized for the rat caudal spine (4-5 mm diameter, 5-6 mm high) were fabricated, seeded with bovine NP cells within a hyaluronic acid hydrogel and bovine AF cells within a layered PCL/poly(ethylene oxide) (PEO) scaffold, and combined with two acellular PCL foam endplates (fig. S1).(21) eDAPS were cultured for 5 weeks in vitro in chemically defined media with TGF-β3 prior to implantation in the athymic rat caudal disc space for either 10 weeks ($n = 5$) or 20 weeks ($n = 9$) with external fixation to immobilize the motion segment and ensure eDAPS retention. (22)

Magnetic resonance imaging (MRI), particularly T2-weighted MRI, is a clinical tool commonly used to assess disc health.(26) Quantitative T2 mapping of the disc has also demonstrated that T2 relaxation times in the NP are positively correlated with disc hydration, proteoglycan content, and mechanics.(27) T2 mapping (Fig. 1A) of implanted eDAPS demonstrated that T2 relaxation times in the NP were maintained at native values after 10 or 20 weeks of in vivo implantation (Fig. 1B). eDAPS AF T2 values, however, were significantly higher ($P < 0.01$) than the native AF at 20 weeks (Fig. 1C). Conversely, endplate T2 values decreased from pre-implantation values at 10 and 20 weeks, suggestive of new matrix deposition in this region (fig. S2). Overall, this MRI data suggested that the

eDAPS maintained their biochemical composition and hydration within the NP and AF with long-term implantation.

MRI results were confirmed via histology and quantitative biochemistry. Alcian blue and picrosirius red stained sections of eDAPS implanted motion segments showed strong and persistent proteoglycan staining in the NP and increasing collagen deposition in the AF from 10 to 20 weeks – recapitulating the matrix distribution of the native disc (Fig. 1D). Evidence of increased integration of the engineered endplate with the native vertebral bodies was also observed with longer durations of implantation. In the native disc, type II collagen and chondroitin sulfate are distributed predominantly within the NP region, with little expression in the AF, which is rich in type I collagen. This distribution of matrix is critical for the mechanical function of the disc – the hydrostatic pressure generated in the proteoglycan-rich and highly hydrated NP places the AF in tension, allowing the disc to bear compressive loads.(28, 29) Immunohistochemistry (fig. S3, fig. S4) revealed similar patterns of matrix distribution within the eDAPS after 10 and 20 weeks of implantation, with robust staining for type II collagen and chondroitin sulfate in the NP region. Type II collagen and chondroitin sulfate staining was lower in the AF region, but was present in the PCL foam endplates, and increased from 10 to 20 weeks. Type I collagen was evenly distributed throughout the eDAPS at both the 10 and 20 week time points.

In accordance with histologic findings, NP, AF, and endplate glycosaminoglycan (GAG) content remained at pre-implantation values over 20 weeks post-implantation (Fig. 1E–G). NP, AF, and endplate collagen content significantly increased ($P = 0.01$, 0.04 and 0.01, respectively) from pre-implantation values after 20 weeks in vivo (Fig. 1H–J). NP and AF GAG and collagen content were generally in the range of the native rat tail NP and AF, with the exception of AF GAG content, which remained below native values at both time points.

These MRI, histology, and biochemistry data demonstrate that the eDAPS composition and hydration are stable over a 20 week period in vivo, and that the eDAPS recapitulate many of the hallmarks of native disc composition and structure. Evidence of maturation of the endplate-vertebral body interface was observed from 10 to 20 weeks implantation. Increased cell infiltration into the AF and endplate regions was evident on histology samples from 10 to 20 weeks, while cells remained within the NP over the same time period (fig. S5, fig. S6). Given that the engineered endplates were acellular at the time of implantation, this suggests that native cells from the adjacent tissues were able to migrate into the open porous structure of the endplate over time and produce matrix.

eDAPS mechanical properties approach native values in vivo.

To elucidate how the observed integration and maturation of the eDAPS in vivo affected spine mechanical function, the compressive and tensile properties of eDAPS implanted motion segments were quantified. After 10 and 20 weeks in vivo, vertebra-eDAPS-vertebra motion segments were isolated and subjected to compressive mechanical testing under physiologic loading (20 cycles compression, from 0 to −3N ~ 0 to 0.25 MPa).(21, 30) This loading regime represents the application of 0.5 times human body weight stress to the engineered disc, the most demanding mechanical testing profile considered to date for any in vivo study of engineered disc implantation, and 16-fold greater than previously used to

characterize the mechanical function of tissue engineered discs after implantation in the rat caudal spine.(19) From these tests, the compressive mechanical properties of the eDAPS implanted motion segments were compared to native rat tail motion segments, as well as the properties of the eDAPS construct after 5 weeks of in vitro culture (pre-implantation).

Marked maturation of eDAPS compressive mechanical properties was observed with increasing duration of in vivo implantation, ultimately matching native motion segment values in most aspects (Fig. 2A). The eDAPS toe region modulus significantly increased ($P = 0.01$) after 20 weeks compared to pre-implantation values, and was not different from the native disc toe region modulus at either 10 or 20 weeks (Fig. 2B). Toe region mechanics in the disc are largely dictated by the function of the NP, suggesting that the NP region continues to mature after in vivo implantation, contributing to overall disc function.(31) The linear region modulus was not significantly affected by in vivo implantation, though there was an increasing trend compared to pre-implantation levels, and implanted eDAPS were not different from the native disc at 10 or 20 weeks in terms of linear region compressive modulus (Fig. 2B). The linear region response of the eDAPS is initially dominated by the PCL comprising the AF region of the eDAPS; as such, native linear region mechanics are recapitulated to some extent even prior to implantation.(21) From histology, it was evident that the PCL within the eDAPS AF persisted over 20 weeks in vivo (Fig. 1D), and therefore likely still contributed to the linear region mechanics at that time point, as new tissue was deposited and accumulated in this region. The eDAPS construct is in an immature state prior to implantation, with low levels of matrix, and the transition and maximum strains of the construct are initially super-physiologic. However, after 10 or 20 weeks in vivo, both transition and maximum strains were significantly reduced ($P < 0.01$) to native values, suggestive of the compositional maturation of the construct and integration with the native tissue (Fig. 2C). Overall, these results demonstrate that eDAPS recapitulate native motion segment mechanical function after long-term implantation, and can withstand the demanding loading environment of the spinal motion segment.

Macroscopic compression testing provides information on the mechanical function of the eDAPS as a whole; thus, the function of the disc region itself (tissue located between the endplates) cannot be determined from this method. As the engineered endplates integrate with the native vertebral body and remodel over time into bone, the engineered disc (DAPS) region will be increasingly responsible for the function of the motion segment. To resolve the mechanical properties of the DAPS, independent of the endplates, mechanics were assessed after 20 weeks in vivo, using a micro-computed tomography (μCT) coupled compression test. For the 20-week implantation group, endplates were rendered radiopaque via the inclusion of zirconia oxide nanoparticles, allowing for μCT visualization of the disc/DAPS boundary. After macroscopic compression testing, vertebra-eDAPS-vertebra motion segments and native rat tail motion segments were subjected to μCT scans before and after the application of a 3N compressive load, representing 0.5 times body weight (Fig. 2D). The height of the engineered disc (DAPS) between the radiopaque PCL endplates and the height of the native disc between vertebral endplates was quantified from pre- and post-compression three dimensional μCT renderings. This analysis enabled computation of strain across the disc itself.(32) Spatial maps of axial disc height (Fig. 2E) revealed similar distributions in disc height across the native disc and DAPS after compression, though the

initial DAPS height was greater than native values. Compressive strain within the DAPS under physiologic compression trended ($P = 0.11$) higher than the native disc (Fig. 2F). This may suggest that, although the macroscopic properties of the eDAPS as a whole recapitulate those of the native motion segment when measured in a dynamic setting, some mechanical insufficiency remains in the disc region of the implant at 20 weeks when measured at equilibrium. This may be due to deficiencies in eDAPS GAG content compared with the native disc, particularly in the AF region.

eDAPS functionally integrate with the native tissue.

Histology, biochemical content and macroscale mechanics suggested progressive integration of the eDAPS with the native tissue after implantation. The extent of this integration was further assessed via second harmonic generation (SHG) imaging, which provides visualization of organized collagen within tissue. SHG signal within the engineered endplates increased substantially from 10 to 20 weeks (Fig. 3A). SHG also demonstrated increasingly robust integration of the eDAPS at both the AF-endplate and endplate-vertebral body interfaces with increasing time post-implantation. Mineralized collagen and sparse vascularization was evident in the engineered endplates at 20 weeks, as observed via Mallory-Heidenhain stained histology sections (Fig. 3B), in which bone matrix stains purple or pink, unmineralized collagen stains blue, and erythrocytes stain orange.(33)

This progressive integration resulted in tangible changes in tensile mechanical properties, which improved from 10 to 20 weeks implantation (Fig. 3C). After compressive macro- and micro-CT based mechanical testing, a complete release of the soft tissue surrounding the eDAPS implants was performed. At 10 weeks, the act of freeing the motion segment from the surrounding soft tissue resulted in failure in one out of three samples. Conversely, all samples in the 20-week group remained intact after circumferential tissue release. When these 20-week eDAPS implanted motion segments were tested to failure in tension, failure occurred at the AF/NP-PCL endplate junction in all samples. In the native rat tail, tensile failure occurred at the growth plate. Increases in the tensile toe region modulus and linear region modulus were evident from 10 to 20 weeks implantation. The toe and linear region moduli (Fig. 3D–E) in tension were within the range of the native rat tail in the 20 week eDAPS implanted motion segments. Failure stress and strain (Fig. 3F–G) of the eDAPS were 46.6% and 50.1% of native values after 20 weeks in vivo, respectively. Tensile properties to failure of a tissue engineered disc after in vivo implantation have not been previously reported. The tensile stresses reached in this study (applying tension to failure) are 45-fold higher than previously reported (675 kPa vs 15 kPa) during non-destructive tensile testing (±3% applied tensile strain) of a tissue engineered disc implanted in the rat caudal disc space.(19)

eDAPS compositionally and functionally mature after implantation in a large animal model.

The results in the rat tail disc replacement model were promising, but rat tail discs are a fraction of the size of a human lumbar or cervical disc, and the rat caudal spine also has a different anatomy and mechanical loading environment compared with the human spine.(34) Thus, clinical translation of the eDAPS requires scale up of the constructs in size and evaluation in a large animal model with comparable geometry and mechanical function to

the human spine. The human cervical spine is a likely first clinical target for a tissue engineered total disc replacement, given that metal and plastic artificial total disc implants have already been used in this location with some success,(35) and it has a smaller size and less demanding mechanical loading environment compared to the lumbar spine. Towards this goal, we chose the goat cervical spine as the large animal model in which to next evaluate eDAPS performance. The goat is a commonly used large animal model for spine research, and the goat cervical spine has the benefit of semi-upright stature and disc dimensions similar to the human cervical spine.(34, 36) We have also recently demonstrated the feasibility of the scale up of DAPS to large, clinically relevant size scales, and illustrated that DAPS sized for the goat cervical disc space compositionally and functionally mature during in vitro culture, albeit at a slower rate than smaller DAPS.(37)

To evaluate our eDAPS in this context, constructs sized for implantation in the goat cervical spine (9 mm high, 16 mm diameter) were fabricated using an agarose hydrogel for the NP region and concentric layers of aligned PCL for the AF region, combined with acellular PCL foam endplates (fig. S1). To use a more translationally relevant cell source for the large animal studies, eDAPS were seeded with allogeneic goat bone-marrow derived mesenchymal stem cells (MSCs) and cultured for 13-15 weeks prior to implantation. The C2-C3 disc space of 7 male, large frame goats was exposed and the native disc and portion of the adjacent vertebral boney and cartilaginous endplate were removed under distraction, using tools commonly used in human cervical spine surgery. The eDAPS was placed within the evacuated space, distraction was released (placing the eDAPS under compression), and the interspace was immobilized with an anterior cervical plate (Fig. 4A–D). Plate fixation was utilized as previous work demonstrated issues with engineered disc retention in the beagle cervical spine without fixation.(20) All goats recovered from the surgical procedure without complication (Fig. 4E), and maintained full cervical spine function (Supplemental Movie 1). Four weeks post-implantation, four animals were euthanized and the cervical spines were harvested for histologic analyses.

After 4 weeks in vivo, Alcian blue and picrosirius red stained mid-sagittal histology sections demonstrated that eDAPS structure was preserved within the goat cervical disc space, and that matrix distribution and content were maintained or slightly improved compared to pre-implantation values (Fig. 5A–B, fig. S7). Histology and SHG images also demonstrated nascent integration of the endplate region with the native tissue. SHG signal was present within the PCL foam, and was contiguous with the signal from the adjacent vertebral body and AF region of the eDAPS, indicative of new organized collagen matrix deposition within the initially acellular PCL foam endplates (Fig. 5C). Additionally, cellularity of the NP and AF regions of the eDAPS was maintained over the 4-week implantation period, and there was evidence of endogenous cell infiltration into the PCL foam endplates. (Fig. 5D, fig. S8). Immunohistochemistry for collagen II, aggrecan, and collagen I demonstrated that the matrix composition of the eDAPS generally recapitulated that characteristic of the native disc, with a collagen II and aggrecan rich NP and an AF composed primarily of collagen I (Fig. 5D, fig. S9). Hematoxylin and eosin staining revealed some infiltration of neutrophils into the outer layers of the eDAPS AF in three of four animals, indicative of a localized mild inflammatory response, potentially due to the allogenic cell source (fig. S8). However, this

was limited to the outermost region of the implant and animals demonstrated no clinical signs of infection, implant rejection, or functional impairment over the study duration.

The remaining three animals were euthanized 8 weeks after implantation, and the eDAPS implants and native goat cervical motion segments were assayed via quantitative MRI and compressive mechanical testing. T2-weighted MRI of eDAPS after 8 weeks implantation demonstrated the maintenance of eDAPS structure in vivo and increased signal intensity in the NP and AF regions compared to pre-implantation values (Fig. 6A–B). Quantitative T2-mapping of the eDAPS implants demonstrated that NP T2 values after 8 weeks implantation were significantly lower ($P = 0.04$) than native T2 values, but were within the range of native healthy goat cervical discs (Fig. 6C). To assess the function of the eDAPS 8 weeks after implantation, vertebra-eDAPS-vertebra motion segments were isolated after removal of the anterior fixation plate and were subjected to compression testing at physiologic loads. The stress applied to the eDAPS was equivalent to that applied to the average human cervical disc space (20 cycles of compression, 0 to 25N, 0 to 0.084 MPa). Mechanical functionality of a tissue engineered disc in vivo in a large animal model has not been previously reported.

eDAPS compressive mechanical properties increased from their pre-implantation values, and either matched or exceeded the compressive properties of adjacent, native cervical discs (Fig. 6D). The toe region modulus was significantly ($P = 0.02$) increased in eDAPS implanted motion segments compared to pre-implantation values (Fig. 6E), whereas transition and maximum strains were significantly reduced ($P = 0.04$ and $P = 0.03$, respectively) from pre-implantation values after 8 weeks in vivo (Fig. 6F). eDAPS moduli and strains were not significantly different from the native cervical disc after 8 weeks in vivo. This maturation of the mechanical properties of the implants is likely due to progressive integration of the eDAPS with native tissue, as evidenced via μCT imaging (fig. S10).

Previous studies have pioneered the translation of tissue engineered discs from the rat tail to the beagle cervical spine; however, the beagle cervical disc space is less than half the size of the human cervical disc space.(20) This previous work in the beagle spine found promising results at 4 weeks; however, loss of proteoglycan content and disc height were evident with longer durations, and mechanical properties following implantation were not reported.(20) Here, we established a goat cervical disc replacement model, which shares similar dimensions to the human cervical spine, and our results demonstrate the feasibility of translation of the eDAPS to this large animal model. eDAPS composition, hydration and cellularity were maintained in vivo, and there was evidence of integration of the eDAPS with the native vertebral bodies. 8 weeks after implantation, the mechanical function of the eDAPS implants was similar to native disc mechanical properties, and demonstrated significant maturation from pre-implantation values.

Discussion

Whole disc tissue engineering holds promise as a treatment strategy for patients with end stage disc degeneration and associated spinal pathology necessitating surgical intervention. Upon implantation in vivo, a successful tissue engineered disc replacement would restore

native disc space height, integrate with the adjacent vertebral bodies, recapitulate the mechanical function of the disc under physiologic loading, and retain a viable cell population to maintain matrix composition and distribution similar to the native, healthy disc. To progress towards clinical translation, tissue engineered discs should ultimately be evaluated using large animal models with comparable geometry, anatomy, and mechanics to the human spine. Tissue engineering of an intervertebral disc for human clinical application has the additional challenge of length scale, with disc heights of 5 mm for the cervical spine and 11 mm for the lumbar spine.(34, 38) The intervertebral disc is also unique in that it is the largest avascular structure in the body, resulting in a low nutrient environment that will also pose a challenge to large-scale tissue engineered constructs.(39)

Given these challenges, the majority of the work in the field thus far has been limited to the in vitro characterization of tissue engineered discs at small size scales (2-3 mm in height and 4-10 mm in diameter).(13, 14, 16, 18, 40–42) Moreover, very few studies have assessed whole tissue engineered discs in vivo within the spine, and when performed, studies have been limited to small animal models.(19–21) To advance the clinical translation of a tissue engineered whole disc replacement, we previously developed tissue engineered discs with and without endplates (DAPS and eDAPS), and evaluated these constructs in vitro at multiple size scales (up to human cervical disc size), and in the short-term in vivo in a small animal model.(21, 22, 37) In this study, we extended this work to evaluate the composition and mechanical function of the eDAPS for up to 20 weeks in vivo in a rat tail disc replacement model, and additionally evaluated eDAPS sized for the human cervical spine in a large animal model for up to 8 weeks.

Results from this study show that the eDAPS mature compositionally over time in vivo in the rat tail, achieving mechanical properties that are similar to the native disc at 20 weeks. The eDAPS functionally integrated with the adjacent vertebral bodies, yielding robust mechanical properties in tension. Functional integration of a tissue engineered disc in vivo has not been previously demonstrated, yet this is a critical benchmark for clinical translation. Since the function of the native disc is primarily mechanical in nature, whereby compressive loads on the spine are supported via the development of hydrostatic pressure within the NP which places the AF collagen fibers in tension (43, 44), the interfaces of the native disc with the adjacent vertebral body are critical for proper mechanical function and are essential to recapitulate in a tissue engineered construct after in vivo implantation.(45) In the eDAPS, improvements in tensile mechanical properties were accompanied by increasing maturation of the eDAPS interfaces, particularly the PCL endplate-vertebral body junction, where infiltrating host cells deposited collagen within the endplates that, over time, began to mineralize and vascularize. Complete vascularization of the engineered endplates will be essential for the long-term success of the eDAPS in vivo.

Building on these promising results in the rat tail, we translated this technology to a larger length scale that would be directly applicable to the human cervical spine, and here demonstrate successful total disc replacement with an eDAPS in the goat cervical spine. We also demonstrate that the eDAPS can be successfully fabricated from bone-marrow derived MSCs, a more clinically relevant cell source for disc tissue engineering compared with AF and NP cells. The goat cervical spine is a particularly attractive pre-clinical model, due to its

semi-upright stature and the similar height and width of the disc space to the human cervical spine.(46) eDAPS sized for the goat cervical disc could be used in a total disc replacement in humans, using the same surgical approach and instrumentation used in our goat model. Results from this implantation illustrate that after 4 weeks, matrix distribution was either retained or improved within these large-scale eDAPS, with evidence of integration of the eDAPS with the adjacent vertebral bodies. Our MRI results suggest that composition at 8 weeks is maintained or improved from pre-implantation values in vivo in the goat cervical spine, and that the compressive mechanical properties of the eDAPS implanted motion segments either matched or exceeded those of the native goat cervical disc. Despite differences in fabrication (MSCs versus native disc cells and agarose versus hyaluronic acid hydrogels), the maturation trajectory of the eDAPS in vivo in the goat spine thus far parallels our findings in the rat model, including progressive maturation of mechanical properties, nascent integration of the PCL endplates, and maintained composition at early time points. However, longer term studies will be necessary to fully characterize the in vivo function of the eDAPS in the goat model.

Our results show great promise for the translation of a tissue engineered whole disc replacement at the human length scale, yet this study is not without limitations. MSC-seeded eDAPS sized for the goat cervical spine had a slower maturation rate during in vitro culture compared with the small, rat-sized eDAPS, yielding constructs with less robust matrix distribution prior to implantation. This may be due to the reduced ability of MSCs themselves to produce matrix compared to native cells when stimulated with TGF-β3 during culture, and due to larger scale engineered tissues maturing at slower rates than smaller scale constructs.(37, 47) Optimization of the in vitro culture of large-scale eDAPS seeded with MSCs, and a thorough analysis of cell viability, phenotype, and host immune response after implantation will be necessary to further advance clinical translation. Additionally, external and internal fixation methods were used here to immobilize the implanted motion segment and ensure retention of the eDAPS. Ex vivo mechanical testing demonstrated that eDAPS mechanical properties matched or exceeded those of the native goat cervical disc, however the in vivo load bearing capacity of the eDAPS without fixation and the effect on whole spine kinematics on long term outcomes remain to be studied. A future iteration of eDAPS design would ideally incorporate a form of temporary or bioresorbable fixation to stabilize the construct until sufficient integration has occurred such that the eDAPS remains in place under physiologic loading.(48) The findings from this current study support continued work in this area, and demonstrate that replacement of the disc with a tissue engineered analog for the treatment of advanced degeneration is feasible and rapidly approaching the state where human translation is possible.

Materials and Methods

Study design.

The objectives of this study were to elucidate the in vivo maturation and mechanical properties of a tissue engineered intervertebral disc with endplates (eDAPS) after implantation in both small (rat caudal spine) and large (goat cervical spine) animal models. We hypothesized that eDAPS would compositionally mature, functionally integrate with the

native tissue over time, and recapitulate native disc mechanical function in these models. All in vivo studies were approved by the University of Pennsylvania IACUC or the Corporal Michal J. Crescenz Veterans' Affairs Medical Center IACUC, and were performed according to the guidelines recommended by these committees. For the small animal studies, eDAPS were implanted in the caudal disc space of male athymic rats with external fixation for 10 ($n = 5$) or 20 weeks ($n = 9$). After motion segment harvest, all specimens were subjected to MRI T2 mapping. Samples were then randomly designated for histology (10w: $n = 2$, 20w: $n = 2$), macroscale mechanical testing (10w: $n = 4$, 20w: $n = 6$), microscale mechanical testing (20w: $n = 4$), and biochemistry (10w: $n = 3$, 20w: $n = 4$). For large animal studies, eDAPS were implanted in the cervical disc space of male large frame goats with internal fixation for 4 ($n = 4$) or 8 weeks ($n = 3$). At 4 weeks, all implanted motion segments were processed for histology. At 8 weeks, all eDAPS implanted motion segments underwent quantitative MRI T2 mapping, and compressive mechanical testing. For both small and large animal studies, the adjacent, native healthy intervertebral discs were utilized as controls. Data were not blinded, and no data were excluded from this study.

Statistical analysis

Statistical analyses were performed in Prism (Graph Pad Software Inc.), with significance defined as $P < 0.05$. All data are shown as mean ± standard deviation. Data were assumed to be non-normally distributed, as sample sizes were too low to test for normality (Shapiro-Wilk normality test). A Kruskal-Wallis test with a Dunn's multiple comparison test was used to assess differences in MRI T2 values, GAG and collagen content, and mechanical properties in tension and compression for eDAPS implanted in the rat tail disc space for 10 and 20 weeks, compared to either native and pre-implantation values. A Kruskal-Wallis test with a Dunn's multiple comparisons was used to assess differences in compressive mechanical properties between goat eDAPS implants before and after 8 weeks implantation, compared to native goat cervical discs. A two-tailed Mann-Whitney test was used to assess statistical differences in strain measured via μCT compression testing between 20 week eDAPS implanted motion segments and native discs, and differences in NP T2 values in 8 week goat eDAPS implants compared to native goat discs.

Supplementary Material

Refer to Web version on PubMed Central for supplementary material.

Acknowledgments:

The authors would like to acknowledge Debra Pawlowski and Jeffrey House from the Corporal Michael J. Crescenz VA Medical Center Animal Research Facility for their assistance with the rat studies, and the veterinary staff at the Penn Vet Center for Preclinical Translation, New Bolton Center, for their assistance with animal care and management during the goat studies.

Funding: This work was supported by the Department of Veterans Affairs (IK1 RX002445, IK2 RX001476 & I01 RX002274), the Penn Center for Musculoskeletal Disorders (National Institutes of Health, P30 AR069619), and the National Institutes of Health (F32 AR072478-01). The contents do not represent the views of the U.S. Department of Veterans Affairs or the United States Government.

References and Notes:

1. Deyo RA, Mirza SK, Martin BI, Back pain prevalence and visit rates: Estimates from U.S. national surveys, 2002, Spine (Phila. Pa. 1976). 31, 2724–2727 (2006). [PubMed: 17077742]
2. Murray CJL, Vos T, Lozano R, Disability-adjusted life years (DALYs) for 291 diseases and injuries in 21 regions, 1990-2010: a systematic analysis for the Global Burden of Disease Study 2010., Lancet 380, 2197–223 (2012). [PubMed: 23245608]
3. Martin B, DEYO RA, Mirza S, Turner J, Comstock B, Hollingworth W, Sullivan S, Expenditures and health status among adults with back and neck problems, JAMA 299, 656–664 (2008). [PubMed: 18270354]
4. American Academy of Orthopaedic Surgeons and the United States Bone and Joint Decade, The Burden of Musculoskeletal Diseases in the United States (American Academy of Orthopaedic Surgeons, Rosemont, IL, 2008).
5. Urban JPG, Roberts S, Degeneration of the intervertebral disc, Arthritis Res. Ther 5, 120–130 (2003). [PubMed: 12723977]
6. Haefeli M, Kalberer F, Saegesser D, Nerlich AG, Boos N, Paesold G, The course of macroscopic degeneration in the human lumbar intervertebral disc., Spine (Phila. Pa. 1976). 31, 1522–1531 (2006). [PubMed: 16778683]
7. Ghiselli G, Wang JC, Bhatia NN, Hsu WK, Dawson EG, Adjacent segment degeneration in the lumbar spine., J. Bone Joint Surg. Am 86–A, 1497–503 (2004).
8. Freeman BJC, Davenport J, Total disc replacement in the lumbar spine: A systematic review of the literature, Eur. Spine J 15 (2006), doi:10.1007/s00586-006-0186-9.
9. Jacobs W, Tuschel A, de Kleuver M, Peul W, Verbout A, Oner C, Total disc replacement for chronic low-back pain, Cochrane Database Syst. Rev 38, 24–36 (2010).
10. Buckland AJ, Baker JF, Roach RP, Spivak JM, Cervical disc replacement — emerging equivalency to anterior cervical discectomy and fusion, Int. Orthop 40, 1329–1334 (2016). [PubMed: 27055447]
11. Kurtz SM, van Ooij A, Ross R, de Waal Malefijt J, Peloza J, Ciccarelli L, Villarraga ML, Polyethylene wear and rim fracture in total disc arthroplasty, Spine J. 7, 12–21 (2007). [PubMed: 17197327]
12. Mizuno H, Roy AK, Zaporojan V, a Vacanti C, Ueda M, Bonassar LJ, Biomechanical and biochemical characterization of composite tissue-engineered intervertebral discs., Biomaterials 27, 362–70 (2006). [PubMed: 16165204]
13. Nerurkar NL, Sen S, Huang AH, Elliott DM, Mauck RL, Engineered disc-like angle-ply structures for intervertebral disc replacement., Spine (Phila. Pa. 1976). 35, 867–73 (2010). [PubMed: 20354467]
14. Lazebnik M, S. M, P. Glatt, L. Friis, C. Berkland, M. Detamore, Biomimetic method for combining the nucleus pulposus and annulus fibrosus, J. Tissue Eng. Regen. Med 5, e179–e187 (2011). [PubMed: 21774081]
15. Hudson KD, Mozia RI, Bonassar LJ, Dose-Dependent Response of Tissue-Engineered Intervertebral Discs to Dynamic Unconfined Compressive Loading., Tissue Eng. Part A 21, 564–572 (2015). [PubMed: 25277703]
16. Martin JT, Gullbrand SE, Mohanraj BG, Ashinsky BG, Kim DH, Ikuta K, Elliott DM, Smith LJ, Mauck RL, Smith HE, Optimization of pre-culture conditions to maximize the in vivo performance of cell-seeded engineered intervertebral discs, Tissue Eng. Part A 23, 923–234 (2017). [PubMed: 28426371]
17. Xu B, Xu H, Wu Y, Li X, Zhang Y, Ma X, Yang Q, Intervertebral disc tissue engineering with natural extracellular matrix-derived biphasic composite scaffolds, PLoS One 10, 1–16 (2015).
18. Iu J, Massicotte E, Li S-Q, Hurtig MB, Toyserkani E, Santerre JP, Kandel R, In Vitro Generated Intervertebral Discs: Towards Engineering Tissue Integration, Tissue Eng. Part A 23, 1001–1010 (2017). [PubMed: 28486045]
19. Bowles RD, Gebhard HH, Härtl R, Bonassar LJ, Tissue-engineered intervertebral discs produce new matrix, maintain disc height, and restore biomechanical function to the rodent spine., Proc. Natl. Acad. Sci. U. S. A 108, 13106–11 (2011). [PubMed: 21808048]

20. Moriguchi Y, Navarro R, Grunert P, Mojica J, Hudson K, Khair T, Alimi M, Bonassar L, Hartl R, Total Disc Replacement Using Tissue Engineered Intervertebral Discs In An In-vivo Beagle Model, PLoS One 12, 1–18 (2017).
21. Martin JT, Gullbrand SE, Kim D, Ikuta K, Pfeifer CG, Ashinsky BG, Smith LJ, Elliott DM, Smith HE, Mauck RL, In Vitro Maturation and In Vivo Integration and Function of an Engineered Cell-Seeded Disc-like Angle Ply Structure (DAPS) for Total Disc Arthroplasty, Sci. Rep 7, 15765 (2017). [PubMed: 29150639]
22. Martin JT, Milby AH, a Chiaro J, Kim DH, Hebela NM, Smith LJ, Elliott DM, Mauck RL, Translation of an engineered nanofibrous disc-like angle-ply structure for intervertebral disc replacement in a small animal model., Acta Biomater. 10, 2473–81 (2014). [PubMed: 24560621]
23. Nerurkar NL, Baker BM, Sen S, Wible EE, Elliott DM, Mauck RL, Nanofibrous biologic laminates replicate the form and function of the annulus fibrosus., Nat. Mater 8, 986–92 (2009). [PubMed: 19855383]
24. Nerurkar NL, Elliott DM, Mauck RL, Mechanical design criteria for intervertebral disc tissue engineering., J. Biomech 43, 1017–30 (2010). [PubMed: 20080239]
25. Bowles RD, Setton LA, Biomaterials for intervertebral disc regeneration, Biomaterials 129, 54–67 (2017). [PubMed: 28324865]
26. Pfirrmann C. W. a., A. Metzdorf, Zanetti M, Hodler J, Boos N, Magnetic Resonance Classification of Lumbar Intervertebral Disc Degeneration, Spine (Phila. Pa. 1976). 26, 1873–1878 (2001). [PubMed: 11568697]
27. Gullbrand SE, Ashinsky BG, Martin JT, Pickup S, Smith LJ, Mauck RL, Smith HE, Correlations between quantitative T2 and T1ρ MRI, mechanical properties and biochemical composition in a rabbit lumbar intervertebral disc degeneration model, J. Orthop. Res 34, 1382–8 (2016). [PubMed: 27105019]
28. Hukins DW, A simple model for the function of proteoglycans and collagen in the response to compression of the intervertebral disc., Proceedings. Biol. Sci 249, 281–285 (1992).
29. Bonnevie ED, Mauck RL, Physiology and Engineering of the Graded Interfaces of Musculoskeletal Junctions, Annu. Rev. Biomed. Eng 20, 403–429 (2018). [PubMed: 29641907]
30. Beckstein JC, Sen S, Schaer TP, Vresilovic EJ, Elliott DM, Comparison of animal discs used in disc research to human lumbar disc: axial compression mechanics and glycosaminoglycan content., Spine (Phila. Pa. 1976). 33, E166–73 (2008). [PubMed: 18344845]
31. Cannella M, Arthur A, Allen S, Keane M, Joshi A, Vresilovic E, Marcolongo M, The role of the nucleus pulposus in neutral zone human lumbar intervertebral disc mechanics, J. Biomech 41, 2104–2111 (2008). [PubMed: 18571654]
32. Boxberger JI, Auerbach JD, Sounok S, Elliott DM, An in vivo model of reduced nucleus pulposus glycosaminoglycan content in the rat lumbar intervertebral disc, Spine (Phila. Pa. 1976). 33, 146–154 (2009).
33. Cason JE, A rapid one-step Mallory-Heidenhain stain for connective tissue., Stain Technol 25, 225–226 (1950). [PubMed: 14782060]
34. Connell GDO, Vresilovic EJ, Elliott DM, Comparison of Animals Used in Disc Research to Human Lumbar Disc Geometry, 32, 328–333 (2007).
35. Coric D, Guyer RD, Nunley PD, Musante D, Carmody C, Gordon C, Lauryssen C, Boltes MO, Ohnmeiss DD, Prospective, randomized multicenter study of cervical arthroplasty versus anterior cervical discectomy and fusion: 5-year results with a metal-on-metal artificial disc, J. Neurosurg. Spine 28, 1–10 (2018). [PubMed: 29087809]
36. Reitmaier S, Graichen F, Shirazi-Adl A, Schmidt H, Separate the Sheep from the Goats, J. Bone Jt. Surg 99, e102 (2017).
37. Gullbrand SE, Kim DH, Bonnevie E, Ashinsky BG, Smith LJ, Elliott DM, Mauck RL, Smith HE, Towards the Scale up of Tissue Engineered Intervertebral Discs for Clinical Application, Acta Biomater. 70, 154–164 (2018). [PubMed: 29427744]
38. Busscher I, Ploegmakers JJW, Verkerke GJ, Veldhuizen AG, Comparative anatomical dimensions of the complete human and porcine spine., Eur. Spine J 19, 1104–14 (2010). [PubMed: 20186441]
39. Urban JPG, Smith S, Fairbank JCT, Nutrition of the intervertebral disc., Spine (Phila. Pa. 1976). 29, 2700–2709 (2004). [PubMed: 15564919]

40. Nesti LJ, Li W-JJ, Shanti RM, Jiang YJ, Jackson W, Freedman BA, Kuklo TR, Giuliani JR, Tuan RS, Intervertebral disc tissue engineering using a novel hyaluronic acid-nanofibrous scaffold (HANFS) amalgam., Tissue Eng Part A 14, 1527–1537 (2008). [PubMed: 18707229]
41. Park S-H, Gil ES, Cho H, Mandal BB, Tien LW, Min B-H, Kaplan DL, Intervertebral disk tissue engineering using biphasic silk composite scaffolds., Tissue Eng. Part A 18, 447–58 (2012). [PubMed: 21919790]
42. Hudson KD, Bonassar LJ, Hypoxic Expansion of Human Mesenchymal Stem Cells Enhances 3D Maturation of Tissue Engineered Intervertebral Discs, Tissue Eng. Part A 23, ten.TEA.2016.0270 (2016).
43. Humzah MD, Soames RW, Human intervertebral disc: structure and function.Anat. Rec 220, 337–56 (1988). [PubMed: 3289416]
44. Hukins DW, A simple model for the function of proteoglycans and collagen in the response to compression of the intervertebral disc., Proc. R. Soc. B Biol. Sci 249, 281–5 (1992).
45. Berg-Johansen B, Fields AJ, Liebenberg EC, Li A, Lotz JC, Structure-function relationships at the human spinal disc-vertebra interface, J. Orthop. Res 36, 192–201 (2018). [PubMed: 28590060]
46. Qin J, He X, Wang D, Qi P, Guo L, Huang S, Cai X, Li H, Wang R, Artificial Cervical Vertebra and Intervertebral Complex Replacement through the Anterior Approach in Animal Model: A Biomechanical and In Vivo Evaluation of a Successful Goat Model, PLoS One 7, e52910 (2012). [PubMed: 23300816]
47. Erickson IE, Huang AH, Chung C, Li RT, Burdick JA, Mauck RL, Differential Maturation and Structure–Function Relationships in Mesenchymal Stem Cell- and Chondrocyte-Seeded Hydrogels, Tissue Eng. Part A 15, 1041–1052 (2009). [PubMed: 19119920]
48. Mojica-Santiago JA, Lang GM, Navarro-Ramirez R, Hussain I, Härtl R, Bonassar LJ, Resorbable Plating System Stabilizes Tissue-Engineered Intervertebral Discs Implanted Ex-Vivo in Canine Cervical Spines, JOR Spine, e1031 (2018). [PubMed: 31463449]
49. Gullbrand SE, Schaer TP, Agarwal P, Bendigo JR, Dodge GR, Chen W, Elliott DM, Mauck RL, Malhotra NR, Smith LJ, Translation of an injectable triple-interpenetrating-network hydrogel for intervertebral disc regeneration in a goat model, Acta Biomater. 60, 201–209 (2017). [PubMed: 28735027]
50. Johnstone B, Hering TM, Caplan a I., Goldberg VM, Yoo JU, In vitro chondrogenesis of bone marrow-derived mesenchymal progenitor cells., Exp. Cell Res 238, 265–272 (1998). [PubMed: 9457080]
51. Martin JT, Collins CM, Ikuta K, Mauck RL, Elliott DM, Zhang Y, Anderson DG, Vaccaro AR, Albert TJ, Arlet V, Smith HE, Population average T2 MRI maps reveal quantitative regional transformations in the degenerating rabbit intervertebral disc that vary by lumbar level, J. Orthop. Res 33, 140–148 (2015). [PubMed: 25273831]
52. Boxberger JI, Auerbach JD, Sen S, Elliott DM, An In Vivo Model of Reduced Nucleus Pulposus Glycosaminoglycan Content in the Rat Lumbar Intervertebral Disc, Spine (Phila. Pa. 1976). 33, 146–154 (2008). [PubMed: 18197098]
53. Martin JT, Gorth DJ, Beattie EE, Harfe BD, Smith LJ, Elliott DM, Needle puncture injury causes acute and long-term mechanical deficiency in a mouse model of intervertebral disc degeneration, J. Orthop. Res 31, 1276–1282 (2013). [PubMed: 23553925]

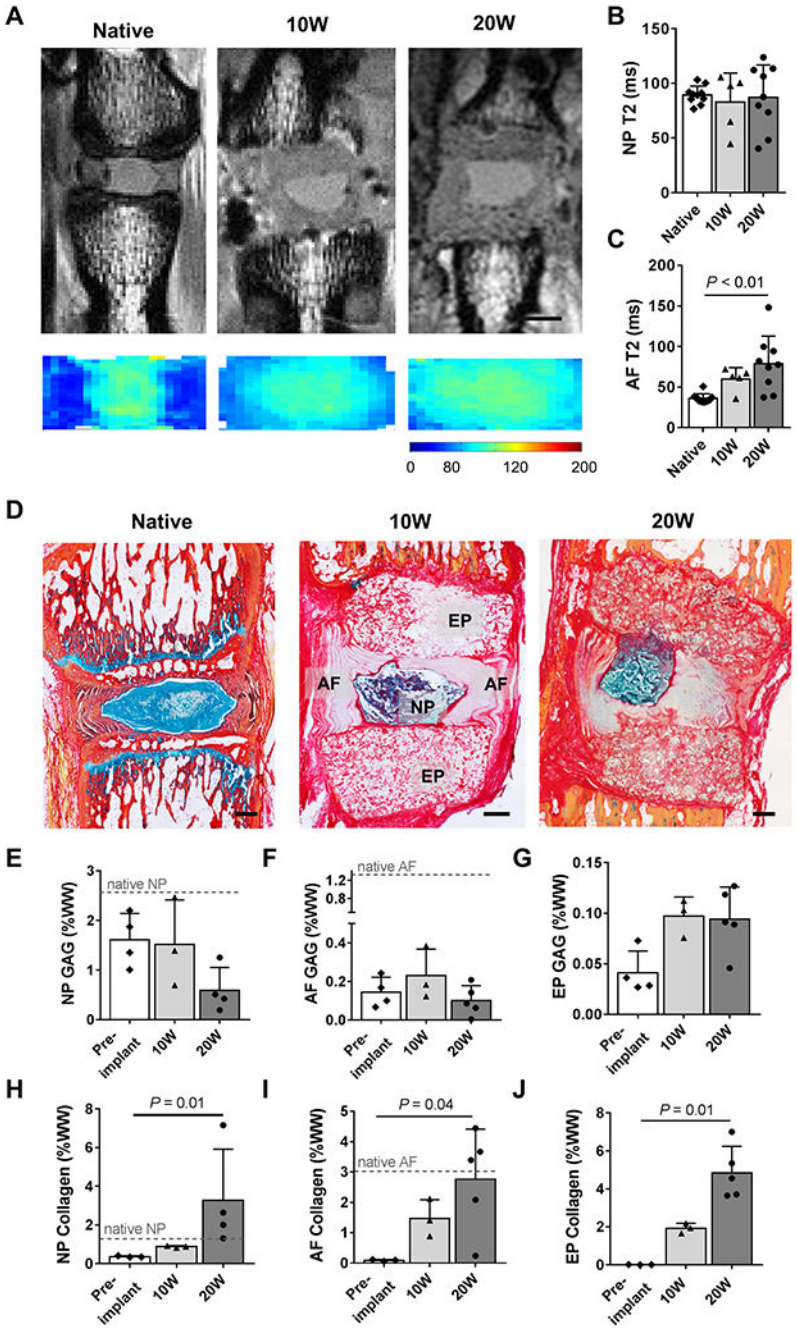

Fig. 1. eDAPS structure and composition after in vivo implantation in the rat tail.

(**A**) Representative raw MR images of the first echo of each treatment group (upper), and average T2 maps (lower) of the native disc and eDAPS implants at 10 and 20 weeks (scale = 2 mm), obtained at 4.7T. Quantification of eDAPS (**B**) NP and (**C**) AF T2 values, bars denote significance ($P < 0.01$). eDAPS biochemical content was further assessed via (**D**) Alcian blue (proteoglycans) and picrosirius red (collagen) stained histology sections of 10 week and 20 week implants compared with the native rat tail disc space (scale = 500 μm). (**E**) Quantification of GAG content in the NP, (**F**) AF and (**G**) PCL endplate regions of the

eDAPS. (**H**) Quantification of collagen content in the NP ($P = 0.01$, 20W vs. pre-implantation), (**I**) AF ($P = 0.04$, 20W vs. pre-implantation) and (**J**) PCL endplate regions of the eDAPS ($P = 0.01$, 20W vs. pre-implantation). Quantitative data are shown as mean with standard deviation ($n = 5$-10 per group for MRI data and $n = 3$-4 per group for biochemistry data). Significant differences between groups were assessed with a Kruskal-Wallis with Dunn's multiple comparisons test.

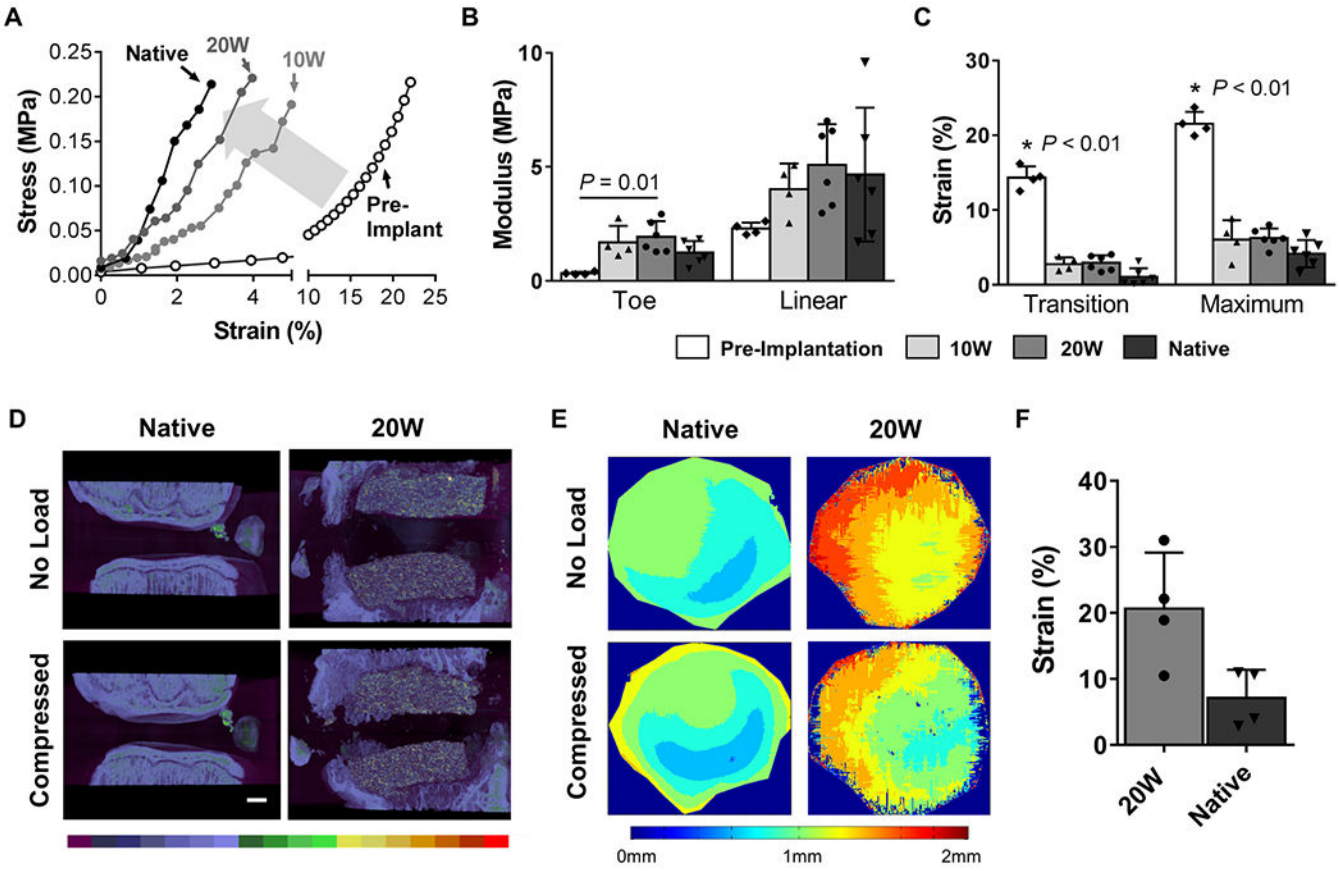

Fig. 2. Compressive mechanical properties of eDAPS implanted motion segments in the rat tail.

(**A**) Representative stress strain curves of eDAPS prior to implantation, and after 10 and 20 weeks of implantation. The shaded arrow highlights the maturation of mechanical properties towards native values. (**B**) Quantification of the toe and linear region modulus *(P* = 0.01, 20W toe modulus vs. pre-implantation toe modulus), and (**C**) transition and maximum strains (* = $P < 0.01$ compared with all groups). Data are shown as mean with standard deviation (n = 4-6 per group). Significant differences between groups were assessed with via Kruskal-Wallis with a Dunn's multiple comparison test. (**D**) μCT scanning before and after the application of physiologic compression in native rat tail motion segments or eDAPS implanted motion segments from the 20-week group. Color scale is representative of bone density. Scale = 500 μm. (**E**) Axial maps of regional disc height generated from the μCT scans via a custom MATLAB code. Color scale indicates local disc height. (**F**) Compressive strain calculated from the average disc height for the native disc and eDAPS under compression. Data is shown as mean with standard deviation (n = 4 per group). Statistical significance between 20W and native strains was assessed via a two-tailed Mann-Whitney test *(P* = 0.11).

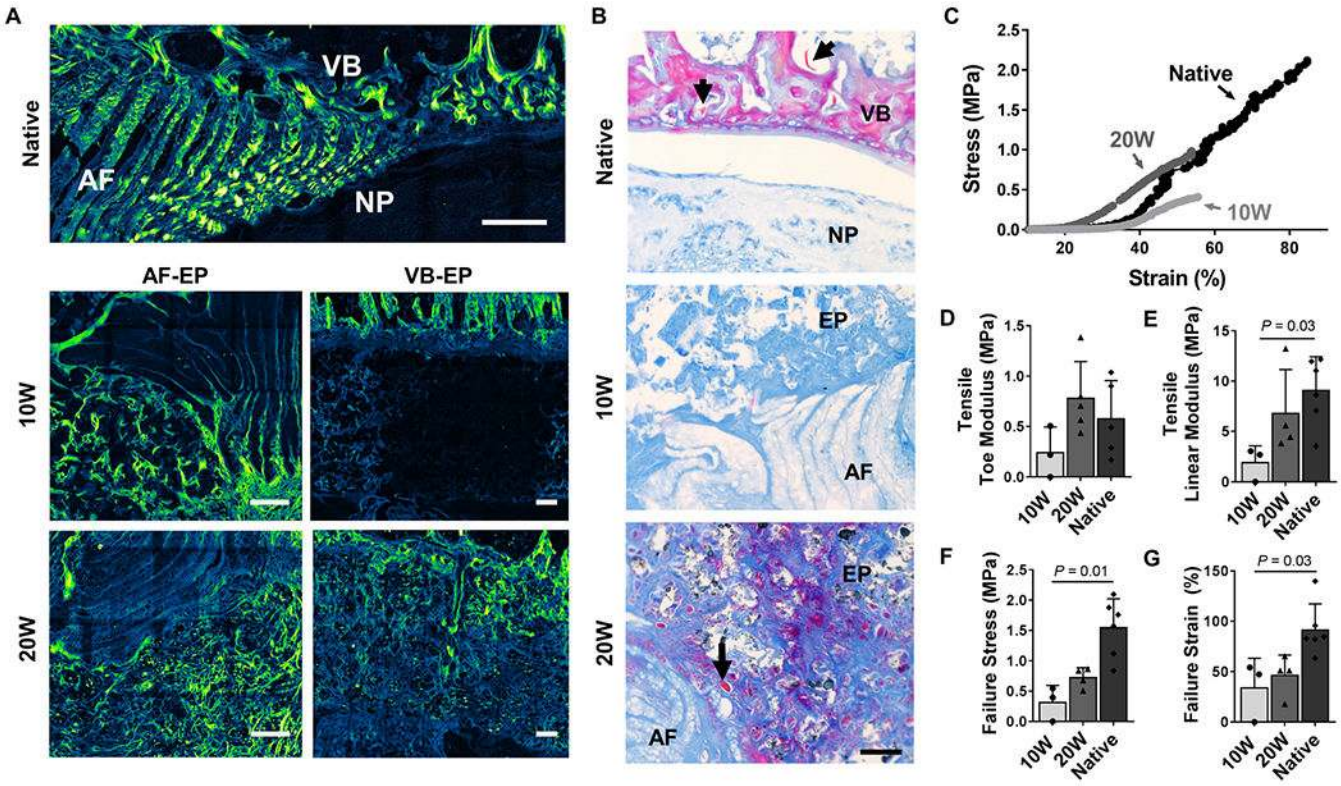

Fig. 3. In vivo integration of eDAPS in the rat tail.

(**A**) Second Harmonic Generation (SHG) images of the AF-endplate and vertebral body (VB)-endplate in eDAPS implanted for 10 and 20 weeks. The AF-vertebral body interface of the native rat tail IVD is shown for comparison. Scale = 200 μm. (**B**) Mallory-Heidenhain stained histology of native rat tail IVD and the PCL endplate regions at 10 and 20 weeks. Bone matrix stains purple/pink, unmineralized collagen stains blue, and erythrocytes stain orange (arrows). Scale = 200 μm. (**C**) Representative stress strain curves from tension to failure tests of eDAPS implanted motion segments compared to native rat tail motion segments. Two out of three motion segments in the 10-week group had quantifiable tensile properties – the remaining sample failed during dissection (represented as "0" data point on graphs D-E). (**D**) Quantification of tensile toe and (E) linear region modulus ($P = 0.03$, 10W vs. native) (**F**) Quantification of failure stress ($P = 0.01$, 10W vs. native) and (**G**) failure strain ($P = 0.03$, 10W vs. native). Quantitative data are shown as mean with standard deviation ($n = 3$-5 per group). Significant differences between groups were assessed using a Kruskal-Wallis with a Dunn's multiple comparison test.

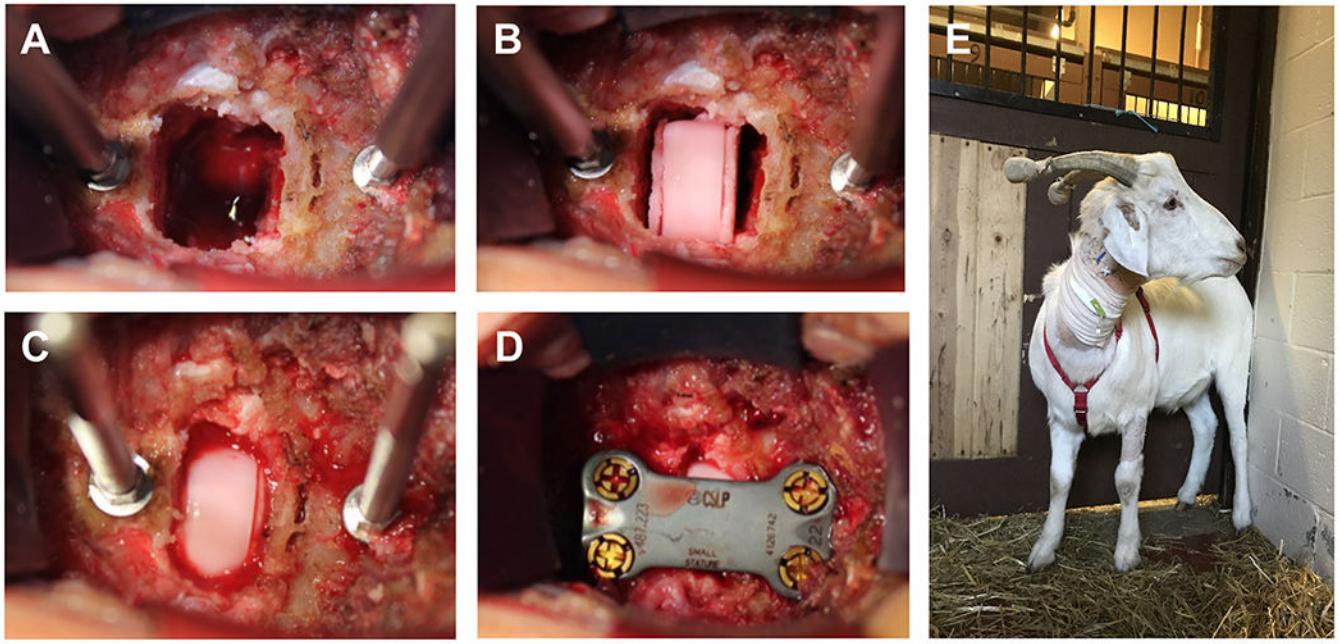

Fig. 4. Translation of eDAPS to a large animal model.

Photographs of eDAPS sized for the goat cervical disc space fabricated and seeded with bone marrow derived allogenic MSCs. (**A**) The C2-C3 disc space was exposed via an anterior approach, and the native disc and portion of the adjacent endplates were removed under distraction. (**B**) 16 mm diameter by 9 mm high eDAPS, pre-matured for up to 13 weeks, were placed within the prepared disc space and (**C**) distraction was released. (**D**) The motion segment was fixed with a cervical fixation plate. (**E**) All animals recovered from the procedure without complication and retained full cervical spine function.

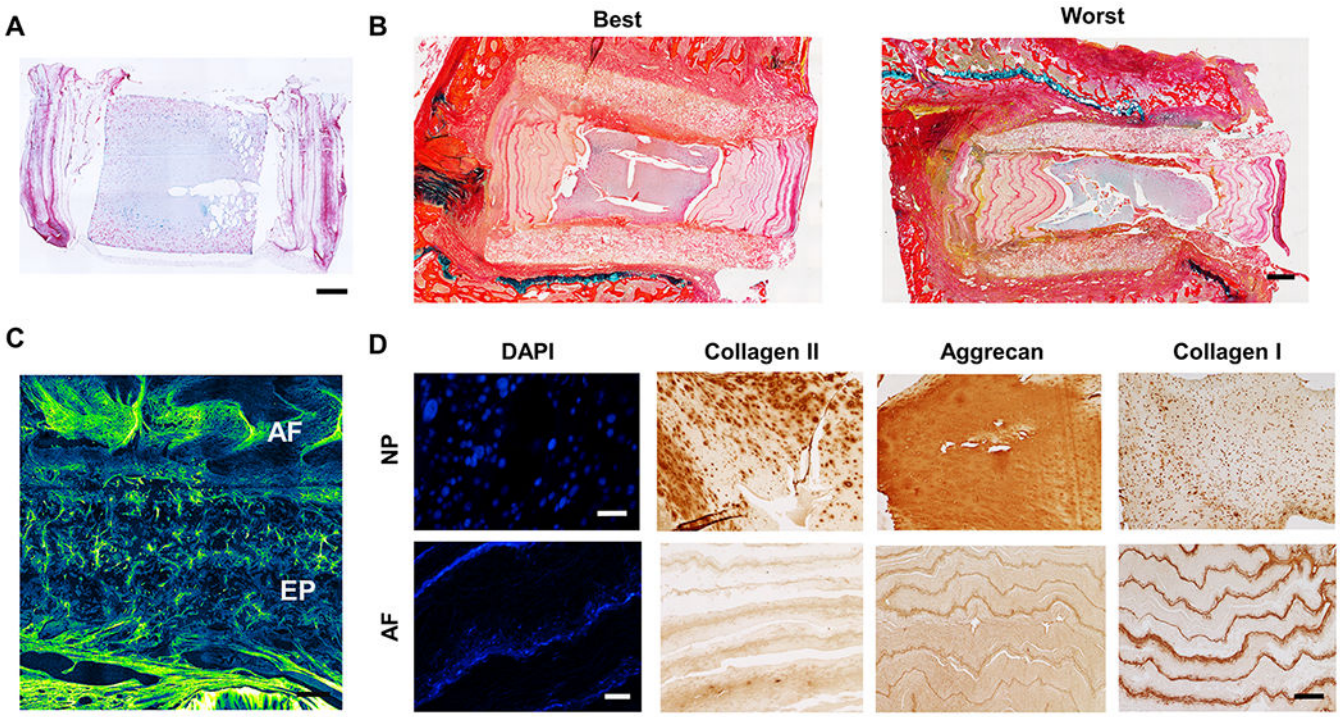

Fig. 5. Four week in vivo performance of eDAPS in a goat cervical disc replacement model.

(**A**) Alcian blue (proteoglycans) and picrosirius red (collagen) stained sections of the eDAPS prior to implantation (after 13 weeks of pre-culture). (**B**) Alcian blue and picrosirius red stained sagittal histology sections 4 weeks post-implantation. Best and worst representative eDAPS are shown. Scale = 1 mm. (**C**) SHG imaging for organized collagen deposition within the PCL endplate, Scale = 200 μm. (**D**) DAPI staining (scale = 50 μm) and immunohistochemistry for collagen II, aggrecan, and collagen I in the NP and AF regions of the eDAPS (scale = 250 μm).

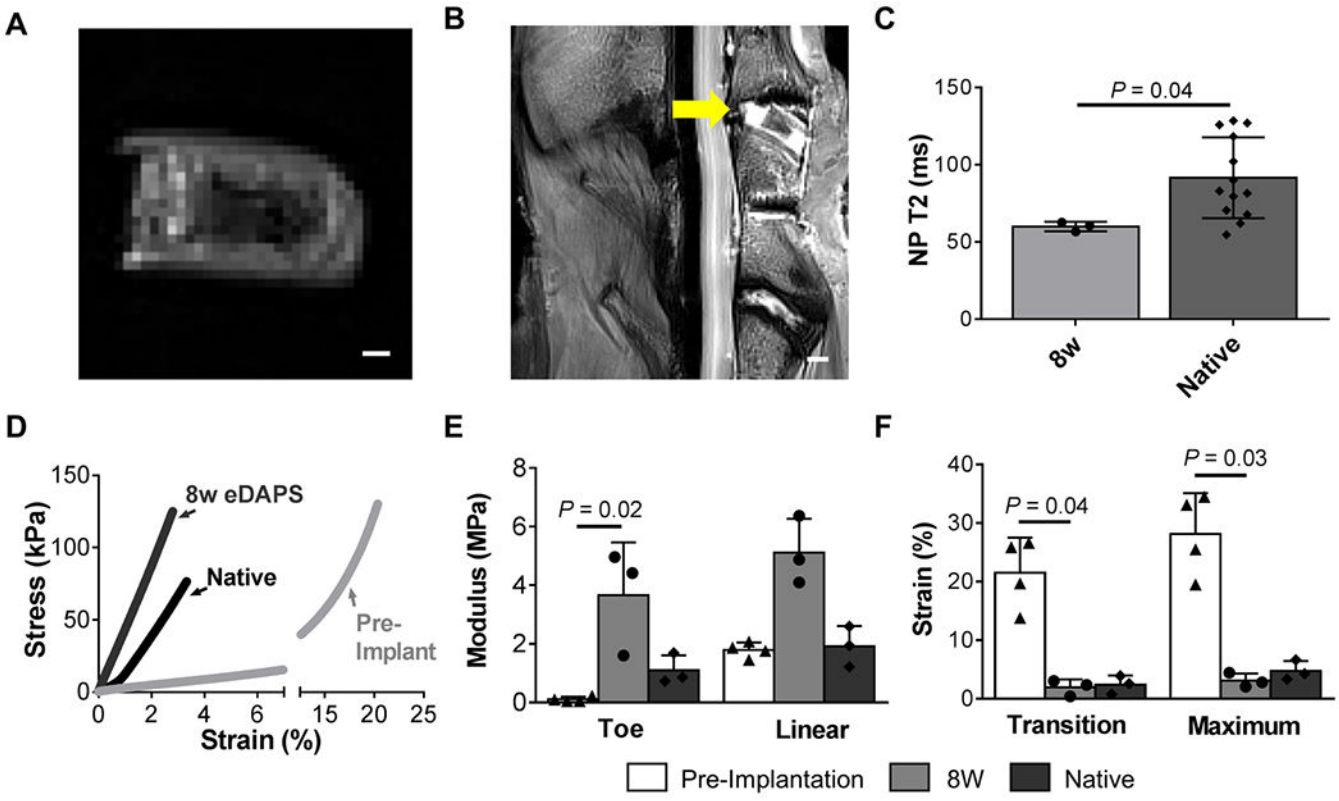

Fig. 6. Eight week quantitative MRI and mechanical properties of eDAPS in a goat cervical disc replacement model.

(**A**) Representative T2-weighted MRIs of eDAPS prior to implantation (scale = 2 mm) and (**B**) 8 weeks post-implantation (arrow, scale = 5 mm). (**C**) Quantification of NP T2 relaxation times in eDAPS implants compared to native goat cervical discs *(P* = 0.04, two-tailed Mann-Whitney test, *n* = 3-13 per group). (**D**) Representative stress-strain curves from compression testing of goat eDAPS before and after implantation, compared to native goat cervical motion segments. (**E**) Quantification of toe and linear moduli of eDAPS implanted motion segments compared to native goat cervical motion segments and eDAPS pre-implantation (*P* = 0.02, pre-implantation vs. 8W toe modulus). (**F**) Quantification of transition and maximum strain in 8 week eDAPS implants compared with native motion segment and eDAPS pre-implantation *(P* = 0.04, 8W vs. pre-implantation transition strain; *P* = 0.03, 8W vs. pre-implantation maximum strain). Quantitative data are shown as mean with standard deviation. Significant differences in mechanical properties between groups (*n* = 3-4 per group) were assessed via a Kruskal-Wallis with Dunn's multiple comparison test.